International Journal of Engineering Innovation & Research
Volume 3, Issue 4, ISSN: 2277 – 5668

Microstructural and Medium Silica Quartz Slurry Erosion Wear Behavior of Silicon Carbide and Zircon Sand Dual Reinforced Particle (DRP) LM-13 Alloy Composites

Surendra Kumar Patel
M. Tech. Scholar, Department of Mechanical Engineering, MANIT, Bhopal, MP, India
Email: surendrakumarptl@gmail.com, Mb.: +919685249465

Sonu Sejkar
M. Tech. Scholar, Department of Mechanical Engineering, MANIT, Bhopal, MP, India

Abstract **– The present investigations are a comparative study the effects of SiC and $ZrSiO_4$ ceramic grain sizes and mixing proportions on the microstructural and slurry erosion wear characteristics of composite materials, SiC / $ZrSiO_4$ dual reinforced particles (DRP) LM-13 alloy matrix composites were manufactured. Dual reinforced particles composites were generated by adding combinations of (9+3)wt%, (6+6) wt.%, (3+9)wt.% silicon carbide (SiC) and zircon sand ($ZrSiO_4$) to an LM-13alloy matrix composite. LM-13 alloy composite with silicon carbide and zircon sand samples were also manufactured for comparison dual reinforcement particles on microstructural features and wear behavior in LM-13 alloy (Al–Si alloy). Silicon carbide (44-53 µm) and zircon sand (20-37 µm) particles are reinforced in the alloy by two-step stir casting method. Slurry erosion wear study reveals that the dual particle reinforcement enhances the wear resistance as compared to single particle reinforcement if mixed in a definite proportion. Study also indicate that a combination of 12 % reinforcement of zircon sand and silicon carbide particles in the ratio of 9,3wt% into the composite exhibits better micro hardness and wear resistance as compared to other combination.**

Keyword **– LM-13 Alloy, Zircon Sand and Silicon Carbide Particles, Microstructure and Micro Hardness, Stir Casting, Slurry Erosion Tester TR-40.**

I. INTRODUCTION

Aluminum alloy matrix composites (AMCs) with multiple reinforcements or hybrid AMCs are finding increased applications in various sectors because of improved mechanical and tribological properties and hence are better substitutes for single reinforced composites [1, 2]. Aluminum and its alloys when reinforced with hard ceramic particulates impart a combination of properties not achievable in either of the constituents individually. Aluminum alloys provide a good matrix for the development of particulate reinforced composites owing to their low density, high specific strength, high corrosion resistance, ease of fabrication, and low cost [3]. In recent years many processing techniques have been developed to prepare particulate reinforced aluminum matrix composites (AMCs). Among the variety of processing techniques available for particulate or discontinuous reinforced metal matrix composites, stir casting is one of the methods accepted for the production of large quantity composites. It is attractive because of simplicity, near net shaping, flexibility and is most economical for large size components to be fabricated. However, it suffers from poor distribution of the reinforcement particles in the aluminum matrix composite. These problems become especially significant as the reinforcement size decreases due to greater agglomeration tendency and reduced wettability of the particles with the melt [4–6]. The dendritic growth and porosity also exists in stir cast composites. Therefore, innovations in processing method of stir casting are of great importance. Stir casting process is modified by various researchers to achieve the desired properties in the composite [7–11]. Two-step stir casting has an advantage in terms of promoting wettability, reduction of porosity, and homogeneous distribution of particles. Moreover, the microstructure is also refined which provide better mechanical properties [9, 10]. In earlier reported two-step stir casting method the mixing of particle is done in semisolid melt by manually stirring with steel rod, which is cumbersome process and also the agglomeration of fine particles occurs. Moreover, mixing is not efficient in reinforcement of fine particle as total volume occupied is increased and semisolid melt solidifies before mixing is completed. In the present study the conventional stir cast processing is bifurcated. In first step the melting and mixing is done properly as is being followed in stir casting and melt is solidified in crucible. In the second step the solidified mass is re-melted for stirring process followed by casting. In recent years numerous research works have been reported on production of multi particle reinforced or hybrid AMCs reinforced with SiC, $ZrSiO_4$, and graphite or in combination of the above, but very limited research work has been done on reinforcement of dual hard particles [2, 12, and 13]. Moreover, no work is reported on slurry erosion wear behavior of LM-13 alloy composites fabricated by stir casting and reinforced with fine silicon carbide (44-53μm) and zircon sand particles (20-37 µm). We investigated the room temperature sliding wear behaviors of reinforced aluminum matrix hybrid composites under both the dry andlubricant conditions. Study shows that wear behavior is related to the fiber orientation of alumina fiber both in dry and lubricated conditions. Suresh and Sridhar [14] studied the dry sliding wear behavior of Al matrix composites reinforced withzircon sand and SiC particulate up to 12 %. Study

International Journal of Engineering Innovation & Research
Volume 3, Issue 4, ISSN: 2277 – 5668

shows that LM-13 alloy/SiC/$ZrSiO_4$ hybrid composite exhibited better wear resistance but optimal addition of graphite particles is necessary. Metal–metal and metal–abrasive wear tests revealed that wear resistance of the composites increased with increasing Mg addition. The present study is aimed to analyze the combined effect of both the hard particles reinforcement in aluminum alloy composite fabricated by modified two-step stir casting. Our study is mainly focused on investigating the microstructural features and wear properties of dual particle reinforced (zircon sand and silicon carbide) LM-13 alloy which has not been studied so far. The effect of dual particle reinforced on the mechanical properties, microstructures, and wear resistance of the particulate reinforced composite at room temperature is reported in this work.

Table 1: Chemical composition of LM-13 alloy

LM-13 alloy	Wt%
Si	11.8
Cu	1.2
Mg	0.9
Ni	0.9
Fe	0.3
Zn	0.2
Ti	0.02
Pb	0.02
Sn	0.005
Mn	0.4
Al	Balance

II. Materials Selection and Experimental Processes

In the present investigation, well-known piston alloy LM-13 alloy is used as matrix material and high purity zircon sand ($ZrSiO_4$) and silicon carbide (SiC) as reinforcement. LM-13 alloy was obtained in the form of ingots. The compositional analysis of the LM-13 alloy was done by wet chemical analysis which is given in Table 1. The composite was made by stir casting route.

Table 2: List of processing parameters

parameters	**1st steps**	**2nd steps**
Melting temperature	800^0C	850^0C
Total stirring time	20mim	4min
Mixing time	8min	-
Blade angle	45^0	45^0
No of blade	4	4
Position of stirrer	Up to 2/3 depth in the melt	Up to 2/3 depth in the melt

Required quantity of LM-13 alloy was taken in a graphite crucible and melted in an electric furnace. The temperature of melt was raised to 800 ^{0}C. This molten metal was stirred using a graphite impeller at a speed 630 rpm. At this 630 rpm vortex is created in the melt, which facilitate to suck the reinforced particles inside the melt.

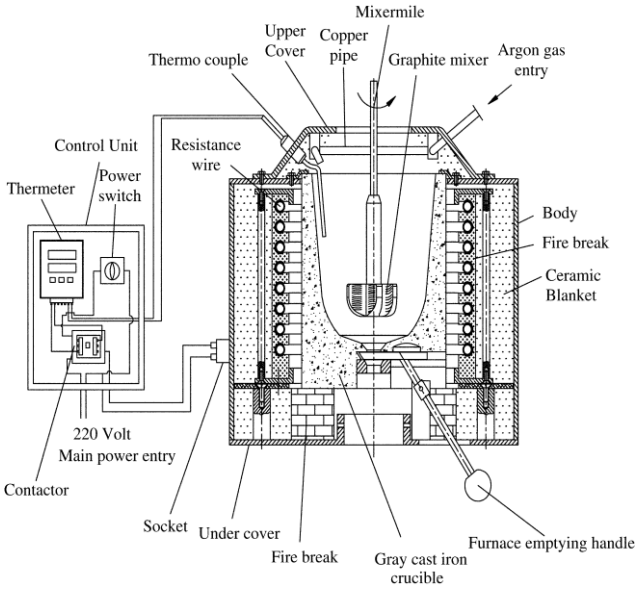

Fig.1. Stirs casting processes

The ceramic particles used as reinforcement were taken in defined proportion and mixed properly by spatula. Particles prior to mixing were preheated at 450^0 C to off the moisture. After the formation of vortex in the melt, the particles were charged inside the vortex at the rate of 20–25 g/min into the melt during stirring by impeller with the help of funnel kept on top of vortex. Zircon sand (20-37µm) and silicon carbide particles of fine grade (44-53 µm) were selected for present work. After mixing of particles the melt slurry is allowed to solidify in a graphite crucible at room temperature conditions. After solidification the mixture is again re-melted in a furnace to ensure that slurry is in fully liquid condition and then melt is stirred with impeller for 12–15 min. similar type of synthesis of composite was reported earlier by various researchers [7, 10, 11]. During production of composite, the amount of LM-13 alloy, stirring duration and position of stirrer in the crucible were kept constant to minimize the contribution of variables related to stirring on distribution of second phase particles. The other detail of it is given in Table 2. In our earlier work it is observed that 12 % reinforcement of zircon sand reinforced composite has given better property, so we have restricted the reinforcement up to 12 % only.In order to compare and correlate the effect of dualparticle reinforcement on mechanical and tribological properties, three different composites containing a total of 12 wt% reinforcement in different proportion were fabricated and have been designated by alphabets. The reinforcement combinations are also given in Table 3.

Table 3: Reinforcement combination of composites

Composite	SiC	$ZrSiO_4$
A	9	3
B	6	6
C	3	9

III. Mechanical Properties of Reinforcement Particles

III.A. Zircon Sand

Zircon sand consists of mostly zircon sand ($ZrSiO_4$) and some hafnium in addition to some rare earth elements, titanium minerals, monazite, etc. Zirconium was found to be a promising candidate as reinforcement material for aluminum, zinc and lead based composites (9).

Table 4: Chemical composition of zircon sand

Composition	ZrO_2	SiO_2	HfO_2	Al_2O_3	Fe_2O_3	MgO
Content (wt%)	67.22	30.85	1.39	0.11	0.029	0.014

Table 5: Mechanical properties of zircon sand

Properties	**Zircon sand**
M.P.(°c)	2500
Limit of application (°c)	1870
Hardness(Moh's Scale)	7.5
Density(g/cm^3)	4.5-4.7
Linear coeff. Of expansion(10^{-6k})	4.5
Fracture toughness(MPa-m$^{1/2}$)	5
Crystal structure	Tetragonal

III.B. Silicon Carbide

Silicon Carbide is the only chemical compound of carbon and Silicon. It is used in abrasives, refractories, ceramics, and numerous high-performance applications. Silicon carbide crystal structure is tetrahedral.

Table 6: Mechanical properties of silicon carbide.

Properties	**Silicon carbide**
M.P. (°c)	2200-2700
Limit of application (°c)	1400-1700
Linear coeff. of expansion (10^{-6k})	4.1-7.7
Density g/cm^3	3.2
Hardness (Moh's scale)	9
Fracture toughness(MPa-m$^{1/2}$)	4.6
Crystal structure	Hexagonal

IV. Microstructure

The microstructural analysis has been completed with the help of scanning electron microscope (JEOL, JSM-6390A, Japan) MANIT, BHOPAL at various magnifications. Before optical observation the sample was mechanicallypolished and etched by Keller's reagent for obtaining better contrast.

V. Micro Hardness

Micro hardness of the different phases was measured (Mitutoyo, japan) using micro hardness tester. Micro hardness measurement was done on each set of sample by taking minimum of five indentations per sample at 100 kgf load.

VI. Slurry Erosion Wear Test

Slurry erosion wear tests of the reinforced alloys composite were performed atSLURRY EROSION TESTER TR-40 under the room temperatures between 25 and 30°C. Before testing, each specimen was ultrasonically cleaned in acetone. The wear tests of specimen from each set of composite have been conducted at the 500, 1000, 1500 rpm and at three different slurry concentration of medium silica quartz sand 25%, 50%, 75% and water by wt% in gms. The test specimens of size 76.5x25.4x6.35 mm were metallographically prepared and polished. Silica quartz medium sand: AFS 40/50 mesh sizes were used as slurry. Test duration of one hour was adopted for all specimens. Using digital weighting machine of accuracy 0.1 mg wear was measured. The mechanical specification details of slurry erosion are given below.

Table 7: Details of the slurry erosion testing apparatus

S.No.	**Details**	**Remarks**
1	No of work stations	6
2	Speed	Variable speed in steps of 1 rpm, min speed 500 rpm, max speed 1500 rpm
3	Test duration	Max 99.59.59 hr: min: sec
4	Base plate height from floor	1085mm
5	Cooling tank lowest height from floor	935mm
6	Travel length of slurry cooling tank	240mm
7	Slurry erosion chamber size	720 x 440 mm
8	Slurry vessel size	Ø120 x120mm depth
9	Slurry height inside vessel	60mm
10	Cooling tank size	720 x 440 x 135mm
11	Water inlet 7 outlet port size	3/8" hose pipe
12	Specimen size	76.5 x 25.4 x 6.35mm
13	Equipment size l x b x h	890 x 835 x 1335mm
14	Weight of equipment	kg

VII. Results and Discussion

VII.A. Microstructure Analysis

The SEM micrograph of the composites is shown in Fig. 5a–c. The micrograph clearly reveals the absence of dendritic morphology in all the composites under investigation. The dendritic structure can be modified during casting which is influenced by many factors such as dendritic fragmentation, restriction of dendritic growth by

the particles, and thermal conductivity mismatch between the particles and melt. Dendritic fragmentation can be attributed to the shearing of initial dendritic arms by the stirring action. It was also found that the perturbation in the solute field due to the presence of particles can change the dendrite tip radius and the dendrite tip temperature. These effects give rise to a dendrite to cell transition as the density of particles is increased. Also the length of the dendrite is reduced in the presence of the particles. Ceramic particle also act as a barrier for dendritic growth and this phenomena is more pronounced if the cooling rate is high. In this work reported that the particle can be assumed to act as a barrier to the dendritic growth.

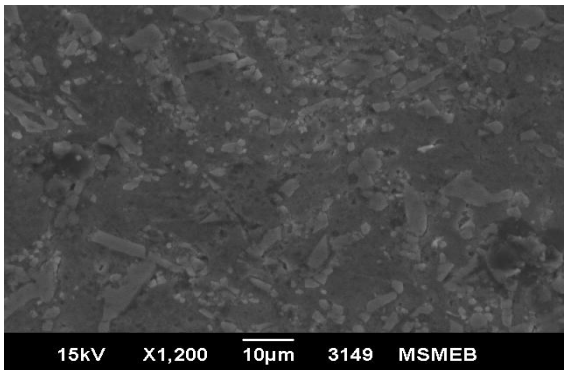

(a)

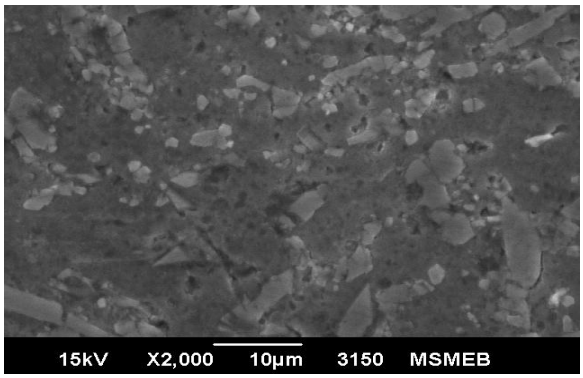

(b)

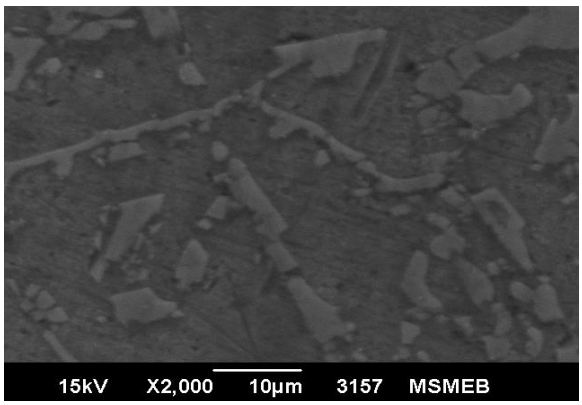

(c)

Fig.2. The SEM micrograph of composites a composite A, b composite B, c composite C

The SEM micrographs of composite 'A' reinforced with 12 % of SiC and zircon sand particles in the ratio of 3:1 are shown in Fig. 2a. Micrograph shows the refined microstructure and homogeneous distribution of particles in the alloy matrix. Refined microstructure and absence of dendritic morphology can be attributed to the two-step stir casting process adopted here in which prolonged time of mixing and stirring is bifurcated. Colonies of eutectic silicon are arranged in the vicinity of the particle. Moreover, near the particle, eutectic silicon having globular morphology or blunted morphology as compared to the matrix can be seen. Each and every particle is having a colony of eutectic silicon which is indicative of the role of particles in nucleating the eutectic silicon. SiC and zircon sand particles provide effective site for nucleation and also restricts the growth of dendrite and modifies the matrix with more refined structure leading to improvement in strength.

The SEM micrograph of composite B shows that dual particle reinforcement in the ratio of 1:1 for SiC and zircon sand particle reinforcement Fig.2b. It depicts the refinement of microstructure and eutectic silicon. Eutectic silicon along with dispersed particles is densely arranged in such a way that they almost cover the entire matrix. The eutectic silicon refines to finer scale and nucleates near particles as colonies. Clustering of particles is observed at some places and some of the clustered particles have chipped out during polishing the samples. However, fine particles have the tendency of clustering though it is not much pronounced in the prepared composites.

The SEM micrograph of composite 'C' containing 12 % of SiC and zircon sand particles in the ratio 1:3 is shown in Fig. 2c. Finer to coarse distribution of eutectic silicon along with homogeneous distribution of particles can be seen. Eutectic silicon colonies around particle are more pronounced in the micrograph. Eutectic silicon distribution is more refined and morphology has changed from acicular to globular around the particles. Also in the matrix the eutectic silicon having blunted morphology as compared to long needle shape or acicular is seen. However, the fine particles and silicon form a network structure because of pushing interface from different nucleation sites. Moreover, the clustering of fine particles at some places is also observed.

Overall analysis of structure indicates that microstructure is refined whereas eutectic silicon are having blunted and globular morphological features. This refinement may lead to better tribological and mechanical properties in the composite. The colonization of eutectic silicon in the vicinity of the particles enhances particle capability of wear resistance. The reinforced particles are uniformly distributed in the alloy matrix. The good bonding between particles and alloy matrix is also revealed in the microstructural analysis. Moreover, porosity is at minimum level and not observed in the optical examination, although clustering is seen at same places in the composite. Microstructure analysis shows that addition of SiC has a pronounced effect on the microstructure and eutectic silicon refinement. The degree

of microstructure and eutectic silicon refinement increases in accordance with the increase of SiC-reinforced particle percentage. The most prominent feature observed in all composite is the absence of dendritic growth which is accounted for two-step stir casting processing of the composites.

VII.B. Micro Hardness and Density

Micro hardness measurement at different phases of composite has been carried out to know the effect of reinforced particulates on the alloy matrix. This is given in Table 4. Micro hardness measurement has been carried out on the embedded reinforced particles as well as in the vicinity of particles and matrix.

Table 8: Microhardness (H_v) and density of composite

Composite	Particle	Interface	Matrix	Density g/cm^3
A	248.03	126.38	91.08	2.715
B	175.10	112.81	62.83	2.732
C	190.43	119.91	66.28	2.747

VII.C. Slurry Erosion Wear Characteristic on Fine Silica Quartz Sand

Slurry erosion test was performed for 1 hour duration at 500,1000,1500 rpm using medium particle sand at various (25%, 50% and 75%) concentrations and following observations were made.

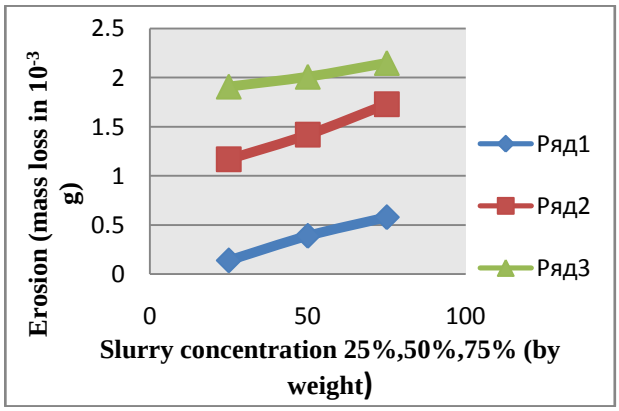

(a)

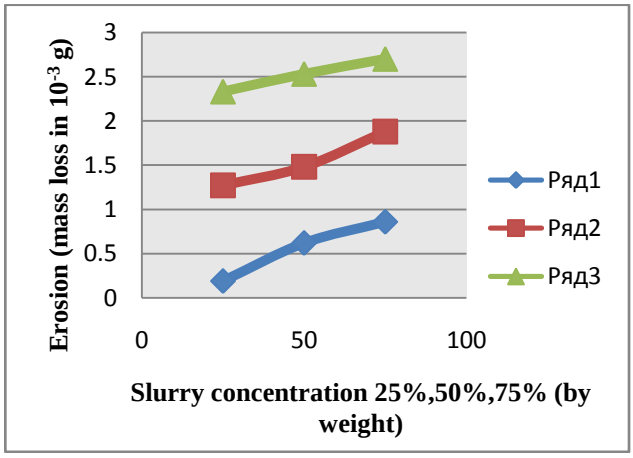

(b)

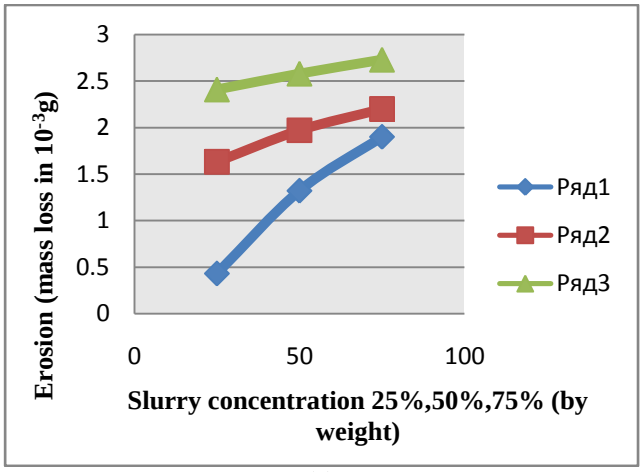

(c)

Fig.3. the mass loss of composites a composite A, b composite B, c composite C at one hour rotation in medium sand (25%, 50% and 75% by weight) at 500, 1000 and 1500 rpm

In above graph series1, series2 and series3 enhance the loss of mass at 500, 1000 and 1500 rpm at various slurry concentrations.

The comparison of slurry erosion wear behavior of all the composites at different speeds (500, 1000 and 1500rpm) and different slurry concentration (25%, 50% and 75% by weight) on medium sand depicts that wear rate increases almost linearly with increase speeds and slurry concentration. It is observed that at low speed and low slurry concentration all the composites exhibit almost similar type of wear behavior. The wear curve trend is almost similar due to speeds and slurry concentration but it is higher for composite B&C and lower for composite A. Good interfacial bonding of reinforcement with the matrix and higher microhardness as possessed by composite a results better wear behavior.

On the other hand, composite a shows better wear resistance at medium silica quartz sand at 500, 1000, and 1500rpm and 25%, 50% and 75% slurry concentration. Wear behavior of composites B and C is nearly similar but run-in wear is higher for composite C. The composite with equal amount of dual reinforcement, i.e., composite B provides better wear properties as compared to composites C. Also the composite A with 75 % silicon carbide and 25 % zircon sand shows increase in wear rate as compared to composite B&C. Dual particles have different role in the matrix, silicon carbide particles refines the eutectic silicon whereas zircon sand particles provides good bonding characteristics to the matrix. zircon sand particles as composite A which shows better wear resistance having combination of 75 % silicon carbide particles and 25 % zircon sand particles. The composite B is combination of 50 % zircon sand and 50 % silicon carbide particles shows better wear resistance as compared to composite C which is composite C having 75 % zircon sand and 25 % silicon carbide particles.

After analyzing wear behavior of composites, it is clear that dual particle reinforcement mixed in definite

proportion is only effective for enhancing wear resistance. Silicon carbide particles are better reinforcement for wear behavior as compared to zircon sand particles. Composite A exhibits better wear resistance due to high microhardness of the interface between particle and matrix.

VII.D. Morphological Analysis of Slurry Erosion Wears Surface

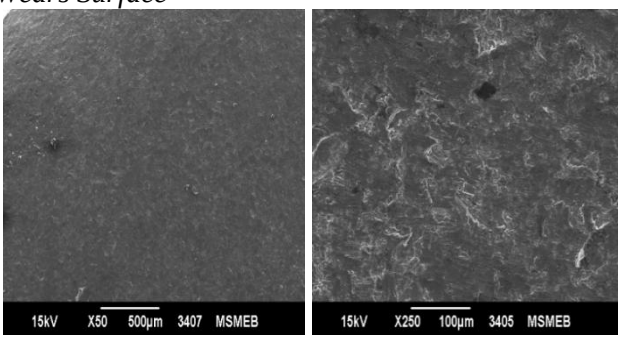

(a) (b)

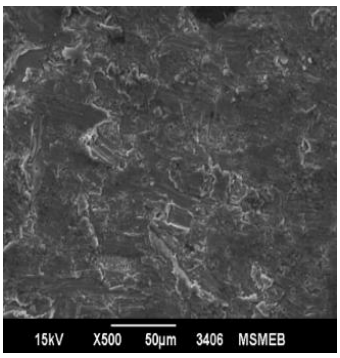

(c)

Fig.4. SEM micrograph of wear surface of composite A at different rpm and slurry concentrations of medium silica quartz sand at different magnifications

The SEM micrograph of wear surface of composite A at different rpm and slurry concentrations of medium silica quartz sand is shown in Fig. 4. Figure 4a corresponds for 5oo rpm which shows the plowing marks with patches. At 500 rpm the plowing marks are not deeper as compared to 1000 and 1500 rpm. The white small particles are also visible, which are originated from the rupture of mechanically mixed layer. At 1000 rpm the craters grow in size as shown in Fig. 4b. The plowing marks become deeper and material removal is accelerated. Figure 4c shows that at 1500 rpm the craters grow in the increasing with loss of material. Several micro cracks are also propagating resulting in the removal of material by delamination. Rupture of mechanically mixed layer accelerated the removal of material by slurry erosive wear.

The SEM micrograph of slurry erosion surface of composite B at different rpm and slurry concentrations of medium silica quartz sand is shown in Fig.5. At 500 rpm composite B is showing high wear rate as shown in Fig. 5a. Long and wider craters along the erosion wear are observed with erosive particles of mechanically mixed layer.

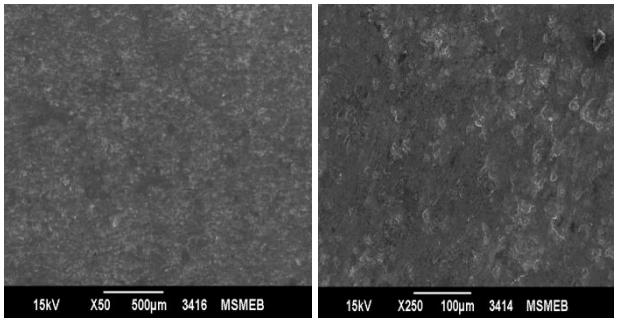

(a) (b)

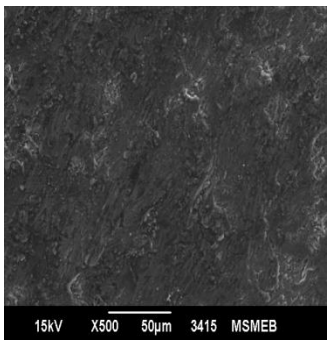

(c)

Fig.5. SEM micrograph of slurry erosion surface of composite B at different rpm and slurry concentrations of fine medium quartz sand at different magnifications

At 1000 rpm the particles of mechanically mixed layer is shown in Fig. 5b. Material removal is excessive as craters become deeper. Flakes of wear surface are also visible in this micrograph. At 1500 rpm the material removal is excessive due to high rpm. The subsurface and surface cracks are visible in Fig. 5c. The crack propagation is along the rpm and slurry concentrations, which result in material removal by delamination. The particles get deboned which results in increase loss of material. we have reported in their work that the first at 25%, to 50% slurry concentration loss of materials increases with increase rpm respectively but at 75% slurry concentration loss of materials decrease as compared to 25%, 50% slurry concentrations. In this way composite A is better wear resistance as compare to composite B.

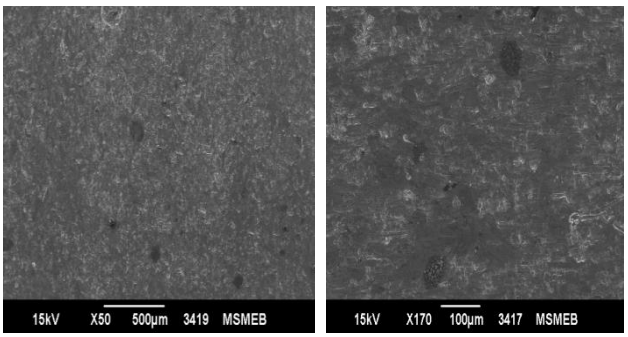

(a) (b)

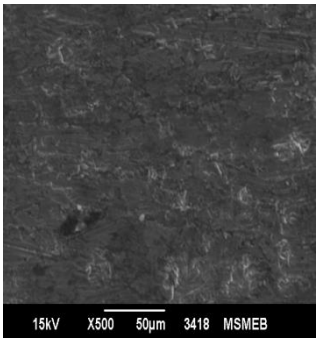

(c)

Fig.6. SEM micrograph of slurry erosion surface of composite C at different rpm and slurry concentrations of medium silica quartz sand at different magnifications

The SEM micrograph of slurry erosion surface of composite C at different rpm and slurry concentrations of medium silica quartz sand is shown in Fig. 6. At 500 rpm composite C is showing high wear rate as shown in Fig. 6a. Long and wider craters along the sliding direction are observed with erosive particles of mechanically mixed layer. At 1000 rpm the particles of mechanically mixed layer is shown in Fig. 6b. Material removal is excessive as craters become deeper. Flakes of wear surface are also visible in this micrograph. At 1500 rpm the material removal is excessive due to high rpm. The subsurface and surface cracks are visible in Fig. 6c. The crack propagation is along the rpm and slurry concentrations, which result in material removal by delamination. The particles get deboned which results in increase loss of material. we have reported in their work that the first at 25%, to 50% slurry concentration loss of materials increases with increase rpm respectively but at 75% slurry concentration loss of materials decrease as compared to 25%, 50% slurry concentrations. In this way composite A is better wear resistance as compare to composite B and composite C.

VIII. CONCLUSION

The present investigation is carried out to determine the influence of dual particle reinforcement on microharnness, microstructural analysis and slurry erosion wear behavior of stir cast (Al–Si alloy) LM-13 alloy composites. The comparison of wear behavior and micro structural micro graphs of the fabricated composite following conclusion can be calculated:

1. The dual particle reinforcement enhances the better erosion wear resistance as compared to single particle reinforcement.
2. Dual particles have different functions in the composite. Silicon carbide refines the eutectic silicon where as zircon sand provides good internal bonding strength.
3. The morphology is not observed in the composites as can be seen in the microstructures of stir cast composites.
4. The combination of reinforcement in aluminum alloy composites 75 % SiC and 25 % zircon sand particles reinforced composite (Composite A) yields better wear resistance as compared to other combination.
5. The reinforcement up to 12Wt% yields better mechanical properties as compared to other combination.

ACKNOWLEDGEMENTS

The authors are thankful to acknowledge the financial support from Maulana Azad National Institute of Technology Bhopal (M.P.) India.

REFERENCES

[1] Alpas AT, Zhang J (1992) J Wear 155:83
[2] Suresha S, Sridhara BK (2010) Mater Des 31:1804
[3] Kaur K, Pandey OP (2010) TribolLett 38:377
[4] Hashim J, Looney L, Hashmi MSJ (1999) J Mater Process Technol 92–93:1
[5] Das S, Udhayabanu V, Das S, Das K (2006) J Mater Sci 41:4668. doi:10.1007/s10853-006-0056-1
[6] Amirkhanlou S, Niroumand B (2010) Trans Nonferrous Met Soc China 20:s788
[7] Manoj S, Deepak Dwivedi D, Lakhvir S, Vikas C (2009) J Miner Mater CharactEng 8:455
[8] Cetin A, Kalkanli A (2008) J Mater Process Technol 205:1
[9] Wang Y, Wang H-Y, Xiu K, Wang H-Y, Jiang Q-C (2006) Mater Lett 60:1533
[10] Zhou W, Xu ZM (1997) J Mater Process Technol 63:358
[11] Hashim J (2001) JurnalTeknologi Dis 35A:9
[12] Bajwa S, Rainforth WM (2005) Wear 259:553
[13] Das S, Das K, Das S (2009) J Compos Mater 43:22
[14] Suresha S, Sridhara BK (2010) Compos SciTechnol 70:1652